Submitted to Annals of Glaciology. 34A119

Revised
545073
21P

Modeled Seasonal variations of firn density induced by steady state surface air temperature cycle

Li Jun,

Raytheon ITSS Code 971, NASA/Goddard Space Flight center, Greenbelt, MD 20771, USA

H. Jay Zwally,

Ocean and Ice Branch Code 971, NASA/Goddard Space Flight center, Greenbelt, MD 20771, USA

ABSTRACT

Seasonal variations of firn density in ice-sheet firn layers have been attributed to variations in deposition processes or other processes within the upper firn. A recent high-resolution (mm scale) density profile, measured along a 181 m core from Antarctica, showed small-scale density variations with a clear seasonal cycle that apparently was not-related to seasonal variations in deposition or known near-surface processes (Gerland and others 1999). A recent model of surface elevation changes (Zwally and Li, submitted) produced a seasonal variation in firn densification, and explained the seasonal surface elevation changes observed by satellite radar altimeters. In this study, we apply our 1-D time-dependent numerical model of firn densification that includes a temperature-dependent formulation of firn densification based on laboratory measurements of grain growth. The model is driven by a steady-state seasonal surface temperature and a constant accumulation rate appropriate for the measured Antarctic ice core. The modeled seasonal variations in firn density show that the layers of snow deposited during spring to mid-summer with the highest temperature history compress to the highest density, and the layers deposited during later summer to autumn with the lowest temperature history

compress to the lowest density. The initial amplitude of the seasonal difference of about 0.13 reduces to about 0.09 in five years and asymptotically to 0.92 at depth, which is consistent with the core measurements.

INTRODUCTION

Seasonal variations of firn density have been observed in numerous field snow-pit and firn-core studies. These variations are more pronounced in the top several meters firn, and generally becoming less significant with increasing depth. Interpretation of the causes of these density variations during firn diagenesis is usually complicated by the variety of changing surface weather conditions. At Plateau station in Antarctica where there is no summer melting, the summer section of each annual firn layer generally consisted of a thin, hard, fine-grained layer, while the winter section was softer, coarse-grained, and more homogeneous than the summer section (Koerner, 1971). However, snow-stratigraphy studies at other polar locations generally showed that summer layers are normally coarser-grained and have lower density and hardness values (e.g. Gow 1961; Benson 1962).

Using improved technology, a very detailed density profile was continuously measured in 3 mm depth intervals along a 181 m core (Gerland and others, 1999). This firn/ice core was from the summit of Berkner Island (79° 36′51″S, 45° 43′28″), Antarctica, which has an annual mean temperature of –27 °C and insignificant summer melting. Such high-resolution measurement provides an excellent and important example for investigating the small-scale characteristics of density evolution during dry-firn densification, which previously has not been satisfactorily explained. In particular, Gerland and others (1999) noted that the measured seasonal cycle, which shows higher densities of summer layers found in the depth below 25 m, was not consistent with observations of higher winter densities in some locations.

Meanwhile, recent analysis of satellite radar altimetry measurements of ice sheet surface elevations revealed seasonal variations in dry firn zones. The observed winter surface is generally higher than the summer surface, with the minimum elevation typically occurring before or near the minimum in summer temperature (Zwally and Li Submitted). This cycle has not been satisfactorily explained either on the basis of seasonal variations in the effective depth of the radar-measurement redundant or by seasonal variations in snow accumulation at the surface. Also, the temperature sensitivity of previous densification models was insufficient to produce a seasonal elevation cycle of sufficient amplitude (e.g. Yi and others 1997).

Our model of surface elevation changes (Zwally and Li, submitted) explained the seasonal surface elevation cycle observed by satellite radar altimeters and produced a significant seasonal variation in firn density profiles. In this study, we apply our 1-D time-dependent numerical model to simulate detailed variations in firn density measured in the Antarctic core by Gerland and others (1999). A principal feature of the model is the temperature-dependent formulation of firn densification that is based on laboratory measurements of grain growth. We use a steady-state surface temperature with seasonal amplitude estimated from a nearby AWS and a constant accumulation rate to drive the model.

THE MODEL

Essential to modeling of the density-depth profile is the rate equation for firn densification. The empirical relation (equation (1)) given by Herron and Langway (1980) is used in the model for calculating the densification rate.

$$d\rho / dt = k A^{\alpha} (\rho_i - \rho) \tag{1}$$

where k is a "rate constant" that is solely dependent on firn temperature (T), A is the mean accumulation rate and exponent α is a constant depending on the stage of densification. Equation (1) has been based on the suggestion that in the densification of firn, the proportional change in air space is linearly related to the change in stress due to the weight (p) of overlying snow (Robin 1958). In equation (1) this weight change is represented by accumulation rate (A) which is normally a function of time (t) i.e. dp/dt = A(t).

The temperature dependence of k follows the Arrhenius-type relation shown by

$$k = k_0 \exp(-E/RT) \tag{2}$$

where R is the gas constant. Both k_0 and the activation energy E have often been used as constants independent of temperature. However, field and laboratory experiments for grain growth and ice creep indicate that the activation energy E for each process is actually a function of temperature (Jacka and Li 1994). Zwally and Li (submitted) incorporated this feature into the model by using the values of E (T) obtained from a best fit curve through the data of activation energy for grain growth. Corresponding $k_0(T)$ values are used to obtain k(T) consistent with the measurements.

The link between the changes in depth and density is given by equation (3). A firn layer is considered with initial thickness determined by the precipitated snow with surface density, ρ_0 in a time span, dt. Equation (1) is applied to each firn layer to calculate the densification rate during dt and thus the density. Assuming the density within each layer is reasonably uniform, for the layer at a depth i and time j the corresponding change (v_{ij}) of the layer thickness (h_{ij}) caused by the density change, is given by

$$v_{ij} = h_{ij}/\rho_{ij}\ (d\rho/dt)_{ij} \qquad (3)$$

The burial depth (z) at any given layer can then be estimated by the sum of the remaining thicknesses of all firn layers at the depth above.

Variations of temperature with time in each firn layer is computed based on the standard heat transfer equation (Paterson 1994)

$$\frac{\partial T}{\partial t} = f(\rho)\frac{\partial^2 T}{\partial z^2} \qquad (4)$$

where f is the thermal diffusivity depending on firn density. We have also used the analytical solution of equation (4) assuming the surface air temperature varies in regular sine function of time with the amplitude T_s (Paterson 1994). The temperature and the density for a firn layer were calculated at the same time.

Equation (1) only takes into account the effects of stress and temperature. The usage of the equation (1) as the constitutive relation to describe the densification process for near surface firn (cm) is rather simplified. Previous studies show that besides other surface processes such wind, solar radiation, temperature gradient (dT/dz) may also accelerate the densification and grain growth in the near surface firn (Alley 1988; Colbeck 1989; Gray and Morland 1995). However these physical processes are more significant in low accumulation area because the intensity of these effects also depends on the duration (determined by accumulation rate) for which the surface firn is subjected to the highly variable surface weather conditions (Nishimura and Maeno 1984). In high accumulation area such as east side of Law Dome Antarctica, these enhanced rates are greatly reduced and the depth hoar layers are hardly developed (Xie and others 1989; Li and others 1990). Therefore our model may be more feasible in the dry snow area with higher accumulation rates where the snow stratigraphy profile is relatively uniform.

RESULTS AND DISCUSSION

The model is driven by the surface air temperature with a regular seasonal cycle and by a constant accumulation rate. Time steps are 30-days. AWS records from two nearby stations AGO-A84 (84.36°S, 23.86°W) and Limbert (75.42°S, 59.95°W), respectively located at higher and lower latitude than the drilling site, show the maximum variation of monthly mean surface temperature is approximately 31° (Linda and others 1996, 1997). Therefore, we use 15.5° as the approximate amplitude (T_s) of the surface temperature with annual mean –27 °C to derive the firn temperature for the drilling site. We also use annual mean accumulation rate 174 kg m^{-2} a^{-1} from the drilling site with surface snow density 300 kg m^{-3} (Gerland and others 1999). Herron and Langway (1980) empirically derived a value of α in equation (1) of approximately 1 for the density below 550 kg m^{-3}, and we use this value as an approximation for the entire density range.

The modeled depth-density profile is compared to the field observation in Figure 1. The shaded area shows the envelope of modeled density variations with depth. Two dashed lines with markers in Figure 1 indicate the range of observed seasonal density variations derived from the mean density profile given by Gerland and others (1999), and a modified curve depth-density variation range for the site (see below). In their core analysis, Gerland and others (1999) found a reverse change of the density variation between 25-50 m along the general decreasing trend of the density variation with increasing depth (density), forming a second peak of the density variation around the depth of 50 m. In this analysis, we consider that this second peak of the density variation is abnormal, which is possibly due to the interannual changes of the surface weather conditions. Changes in physical properties of ideal dry firn during densification more likely follow a continuous trend. By following the general trend of Gerland and others (1999, Fig. 4), a modified curve showing the range of seasonal variation of measured density with depth for the site is given in Figure 2 as indicated.

As shown by Figure 1, our modeled density depth-profile follows the observation with similar range of density variation that declines with increasing density or depth. However, it is evident from Figure 2 that the modeled density variation does not match the observed curve perfectly. In particular, the modeled densification rate exceeds the observed rate before the density reaches approximately 500 kg m^{-3}, although the modeled density appears to be within the range of observed density variations. Besides any imperfections in the model, it should be noted that the observed density variations may bias to its steady state profile due to the possible interannual changes of surface weather conditions.

After the detailed examination of the density data, Gerland and others (1999) indicate that the variations in firn density shown by Figure 1 are actually seasonal. The magnitude of these seasonal variations decreases continuously with depth. This feature of seasonal variation in firn density has been well modeled in our results. Figure 3 presents in larger scale the modeled density variations for the first 10 m shown in Figure 1. The magnitude of the variation decreases with depth as indicated by Figures 1, 2, and 3. This characteristic of the seasonal variation in firn density also agrees well with the field findings at Plateau station in Antarctica (Koerner, 1971).

To examine the specific seasonality in the density variation, we follow the density evolution for each firn layer deposited at 30-day time intervals within a one-year surface temperature cycle, as shown by Figure 4. The densification history of three selected firn layers together with its corresponding temperature history following deposition is shown in Figure 5. As shown by Figure 4, firn layer zero (C0) is deposited in early spring approximately three months prior to the maximum summer temperature. This snow begins to densify at a higher rate as the temperature increases following deposition. Firn layer 5 (C5) is deposited in autumn about two months after the maximum summer temperature. Layer C5 densifies a little while the temperature is in mid-cycle after the deposition, as indicated by the small step of the density curve. However, with the fall in temperature toward winter, the densification is essentially quenched until the next warm season starts in spring. The second step in density of C5 is smaller than the first step for layer C0 deposited in the warm season, because C5 is insulated some by the winter deposited snow. This autumn snow obtained the least density of any of the 30-day layers. Snow deposited in winter obtains a density between these two extremes as shown by the third diagram for layer C11.

The longer period histories of temperature for firn layers C0 and C5 in Figure 6 show that after subsequent seasons the temperature histories of the maximum and minimum density layers are not much different. Clearly, the temperature history of a layer during the first seasonal cycle is the primary determinant of the initial densification, which then remains correspondingly high or low as densification continues. The densification history for the

12 seasonal layers in Figure 7 shows that layers C0 to C3 and layers C11 to C12 that are deposited when temperature is increasing (i.e. dTs/dt >0) obtain higher densities than layers C4 to C9 that are deposited when the temperature is decreasing (dTs/dt <0). Therefore, it is the spring through early summer layers that obtain the highest densities and the autumn through early winter layers that obtain the lowest densities.

CONCLUSION

The high resolution density profile of 181m core retrieved from the summit region of Berkner island Antarctica provides an excellent example of firn densification, especially the seasonal scale density variations detailed to seasonal scale. We believe that the model presented here provides a good description of the densification process that leads to the observed seasonal cycle in firn. The surface temperature cycle is sufficient to generate the seasonal variations in density profile that is observed in dry polar firn. The maximum densities occur in the firn layers deposited during late spring to early summer and minimum densities in those deposited in autumn to early winter.

REFERENCES

Alley, R.B. 1988. Concerning the deposition and diagenesis of strata in polar firn. *J. Glaciol.*, **34**(118), 283-290.

Benson, C. S. 1962. Stratigraphic studies in the snow and firn of the Greenland ice sheet. *SIPRE* Res. Rep. 70.

Colbeck, S.C. 1989. Snow-crystal growth with varying surface temperatures and radiation penetration. *J. Glaciol.*, **35**(119), 23-29.

Gerland, S., H. Oerter, J. Kipfstuhl, F. Wilhelms, H. Miller and W.D. Miners. 1999. Density log of a 181 m long ice core from Berkner Island, Antarctica. *Ann. Glaciol.*, **29**, 215-219.

Gray, J.M.N.T., and L.W. Morland. 1995. The compaction of polar snow packs. *Cold Reg. Sci. Technol.*, **23**, 109-119.

Gow, A. J. 1961. Drill hole measurements and snow studies at Byrd Station, Antarctica. *SIPRE Tech. Rep.* 78.

Herron, M. M. and C.C. Langway, Jr. 1980. Firn densification : an empirical model. *J. Glaciol.*, **25**(93), 373-385.

Jacka, T. H. and Li Jun, 1994. The steady-state crystal size of deforming ice.. *Ann. Glaciol.*, **20**, 13-18.

Keller, L.M., G.A. Weidner, C.R. Stearns, M.T. Whittaker and R.E. Holmes. 1999. *Antarctic automatic weather station data for the calendar year 1996*. Madison, WI, University of Wisconsin. Space science and Engineering center.

Keller, L.M., G.A. Weidner, C.R. Stearns, M.T. Whittaker and R.E. Holmes. 2001. *Antarctic automatic weather station data for the calendar year 1997*. Madison, WI, University of Wisconsin. Space science and Engineering center.

Koerner, R.M. 1971. A Stratigraphic Method of determining the snow accumulation rate at Plateau Station, Antarctica, and application to South Pole--Queen Maud Land Traverse 2, 1965—1966. *In Crary, A.P., ed. Antarctic snow and ice studies II.* Washington, DC, American Geophysical Union, 225-238. (Antarctic Research Series 16.)

Li, J., N.W. Yong and P.F. Malcom. 1990. Grain growth in firn on Law Dome ice cap, East Antarctica. *Antarctic Res.*, **2**(4), 11-23.

Nishimura, H., and N. Maeno. 1984. Snow structure and depth hoar formation in Mizuho Plateau, Antarctica. *Mem. Natl Inst. Polar Res. Special Issue*, 34, 137-146.

Pasterson, W.S.B. 1994. *The physics of Glaciers. Third edition.* Oxford, etc., Elsevier.

Robin, G. de Q. 1958. Glaciology. III. Seismic shooting and related investigations. *Norwegian-British-Swedish Antarctic Expedition, 1949-52. Scientific Results.* **5**.

Yi, D., C.R. Bentley and M.D. Stenoien. 1997. Seasonal variation in the apparent height of the East Antarctic ice sheet. *Ann. Glaciol.*, **24**, 191-198.

Zwally, H.J. and Li Jun. 2001. Seasonal and Interannual Variations of ice sheet surface elevation at the Summit of Greenland: observed and modeled. *J. Glaciol.*, Submitted [01J028].

FIGURE CAPTIONS

Figure 1. Comparison of modeled and observed depth-density profiles for Summit of Berkner island, Antarctica. Dark area shows the envelope of modeled density variation. Dashed lines with markers indicate the range of observed density variation modified from Gerland and others (1999).

Figure 2. Modeled (solid line) and observed (broken line) range of density variation versus depth for Summit of Berkner island, Antarctica. Data shown by the broken line are modified from Gerland and others (1999).

Figure 3. Seasonal variations in firn density shown by modeled depth-density profile for Summit of Berkner island, Antarctica.

Figure 4. One year surface air temperature (30 day mean) cycle in each 30 day time span. The figure beside each marker indicates the number of the 30 day from the beginning of the year corresponding to the time of deposition of the modeled layers.

Figure 5. Densification history of three selected firn layers together with the temperature history experienced by the corresponding firn layer (cf. numbers in Figure 4). Late-winter layer C11 and early-spring layer C0 obtain higher densities than late autumn layer C5 (lowest density).

Figure 6. Modeled temperature profiles showing the decrease of amplitude of firn temperature experienced by layers (C0 dashed line and C5 solid line) while the

firn layers travel downwards as implied by the changes with time. After the first year the temperature histories are similar.

Figure 7. Sequence of the density history for each snow layer indicated in Figure 4 showing the seasonal variations of the density in each seasonal firn layer.

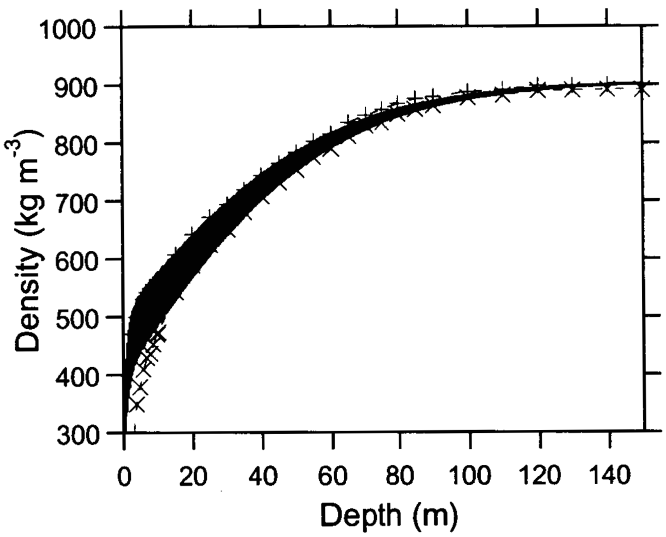

1000
900
800
700
600
500
400
300
Density (kg m-3)
0
20
40
60
80
100
120
140
Depth (m)

Fig. 1

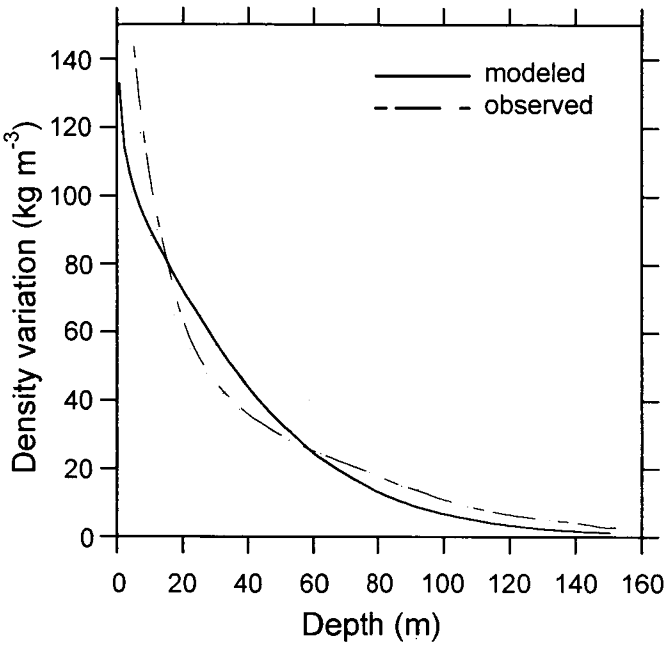
modeled
observed
Density variation (kg m-3)
Depth (m)
0
20
40
60
80
100
120
140
160

Fig.2

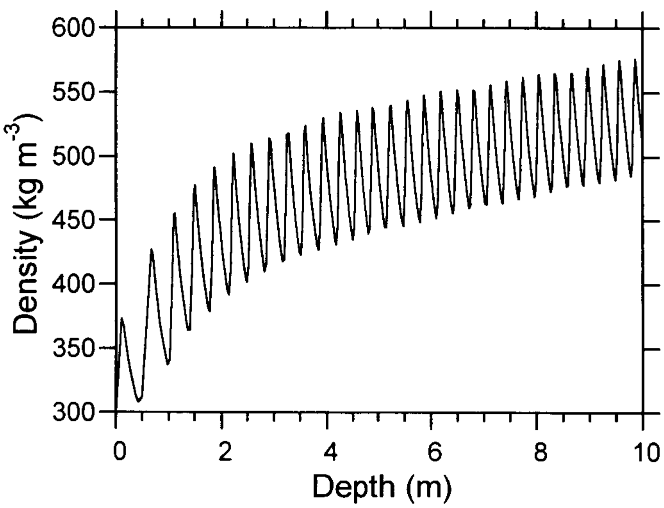

Fig. 3

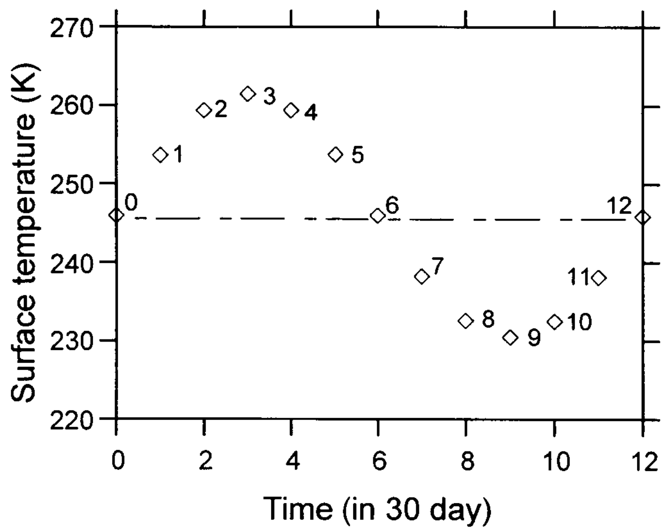

Surface temperature (K)
270
260
250
240
230
220
0
2
4
6
8
10
12
Time (in 30 day)
0
1
2
3
4
5
6
7
8
9
10
11
12

Fig. 4

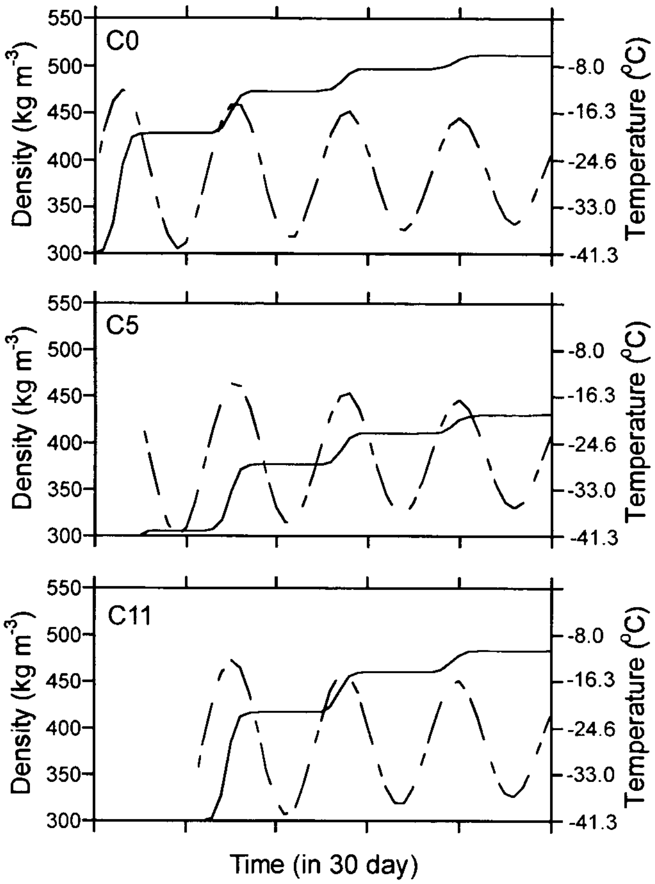
C0
C5
C11
Density (kg m-3)
Temperature (°C)
550
500
450
400
350
300
-8.0
-16.3
-24.6
-33.0
-41.3
Time (in 30 day)

Fig5

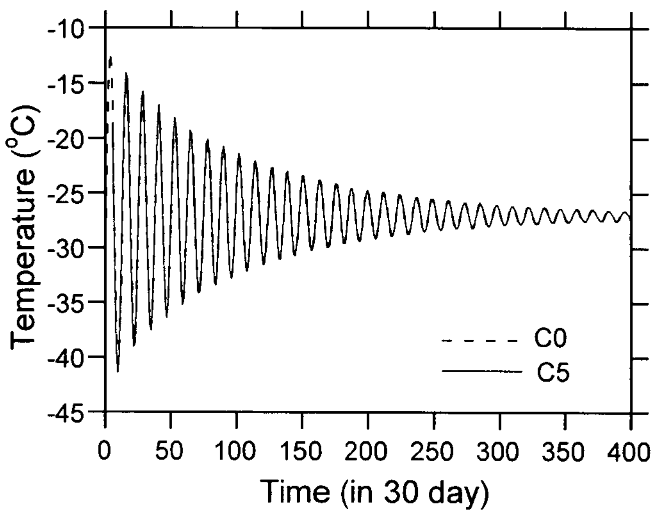

-10
-15
-20
-25
-30
-35
-40
-45
Temperature (°C)
0
50
100
150
200
250
300
350
400
Time (in 30 day)
C0
C5

Fig. 6

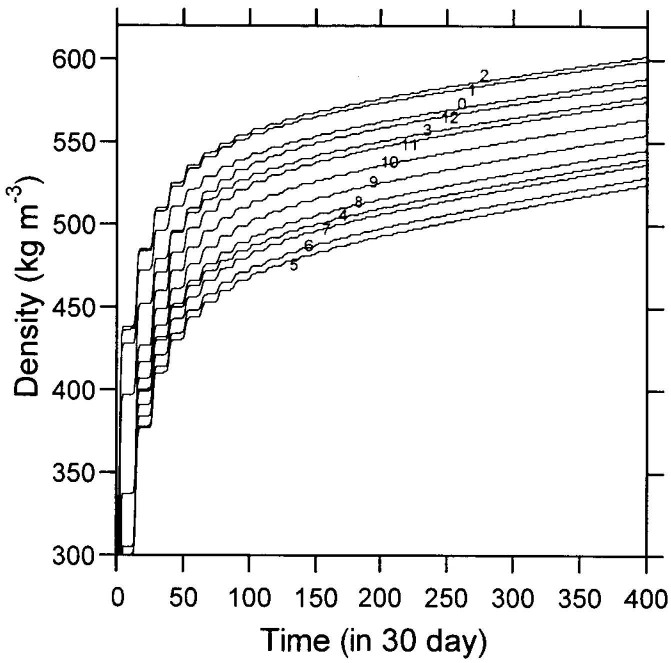

600
550
500
450
400
350
300
Density (kg m^{-3})
0
50
100
150
200
250
300
350
400
Time (in 30 day)
2
1
0
12
3
11
10
9
8
4
7
6
5

Fig.7